Resonances in ultracold collisions of ^{6}Li, ^{7}Li, and ^{23}Na

A.J. Moerdijk, B.J. Verhaar, and A. Axelsson*
Eindhoven University of Technology, Box 513, 5600MB Eindhoven, The Netherlands
(Received 1 February 1995)

We investigate the resonance properties of ultracold ground state ^{6}Li+^{6}Li, ^{7}Li+^{7}Li, and ^{23}Na+^{23}Na collisions. The locations of various resonances and their corresponding error bounds due to the uncertainty of the interatomic potentials are presented. Also, the resonance widths are computed using rigorous coupled-channel calculations, as well as a modified version of Feshbach theory valid for strong fields.

PACS number(s): 32.80.Pj, 42.50.Vk

I. INTRODUCTION

Laser cooling of neutral atoms continues to be a rapidly growing field of activity with a remarkable diversity of new methods and applications. Illustrative of this diversity are recent developments such as gravitational Sisyphus cooling [1], rf-induced evaporative cooling [2], and three-dimensional velocity-selective coherent population trapping [3]. The past year has also shown a rapid development in the determination of the long range interactions between atoms by photoassociation of ultracold atoms [4] and by measuring the highest bound levels of the ground state potentials [5]. One of the crucial quantities searched for is the elastic scattering length, which governs the stability of the condensate in Bose-Einstein condensation experiments: it must be positive in order to give a stable condensate. In [6] it was found that for specific values of the magnetic field, resonances in the scattering length show up. These resonances offer the possibility to change the value of the scattering length and allow one to make it not only positive but also large, a condition for efficient evaporative cooling [24]. Apart from this, resonance behavior in ultracold collisions is interesting on its own. Resonances would undoubtedly give rise to fascinating phenomena; in particular, the structure of the two-particle correlation function will be totally different locally or over the whole gas sample in the trap, with associated consequences for the gas properties (e.g., equation of state). Furthermore, knowing the exact positions of the resonances allows one to extract the positions of the highest bound levels of the S=0 singlet and S=1 triplet potentials, which by their proximity to the continuum threshold greatly help to reduce the uncertainty about the interactions of ultracold atoms.

In a recent search for these s-wave scattering resonances in ^{87}Rb [7], unfortunately none were found. The problem with the heavier alkali atoms such as rubidium and cesium is that the ground state potentials are not sufficiently known to theoretically predict the positions of the resonances. In the case of Li and Na, however, we believe the potentials to be accurate enough for this purpose. In this paper we briefly review the Feshbach theory of resonances in the light of ultracold atom collisions and look for the positions of resonances for the collisions of various diatom combinations. Apart from the bosonic species ^{7}Li and ^{23}Na we also consider the fermion ^{6}Li. As is well known, ultracold collisions have characteristic properties for fermionic atoms. Antisymmetry requires the system to have odd collisional orbital angular momentum if we are considering atoms in the same spin state. As the number of partial waves needed to describe a scattering process decreases with the kinetic energy, for sufficiently low energy the interaction will be almost exclusively p wave. This means that a centrifugal barrier will keep the atoms apart, reducing the nonresonant phaseshift (potential scattering) almost to zero. Any resonances will therefore show up clearly, approaching the ideal Breit-Wigner shape without interference from a background phase shift.

II. COLD COLLISIONS IN TRAPS

A common way to trap neutral atoms is to use a static magnetic field. One drawback is that it is impossible to create a local maximum for a static electromagnetic field in free space. One is therefore limited to atomic (hyperfine) states that are low-field seeking over some range of the external field. A more recent technique involves the use of a microwave field, which avoids the restriction to low-field seeking states imposed by a static field. The microwave trap has been demonstrated in the past year for cesium [8]. Another trapping method where one is not limited to specific hyperfine states is the far-off-resonance optical dipole trap [9]. An interesting recent proposal is trapping atoms by means of focused high power infrared lasers [10], which would make it even possible to trap different atomic species simultaneously and study their mutual collision properties.

Cold collisions are commonly described by the coupled-channel method [12,13]. The effective total Hamiltonian of the system is written as the sum of a part H_0 with

*Present address: Uppsala University, Thunbergsvägen 3, S-752 38 Uppsala, Sweden.

eigenstates $|\{\alpha\beta\}\rangle$ (so-called channels) tending asymptotically to a single symmetrized separate-atom product of internal states $|\alpha\rangle$ and $|\beta\rangle$ and an interaction part V coupling the channels. Expanding the total scattering state Ψ in this basis with $\vec{r}$-dependent coefficients

$$\Psi = \sum_{\{\alpha\beta\}} \psi_{\{\alpha\beta\}}(\vec{r})|\{\alpha\beta\}\rangle \tag{1}$$

and substituting this in the Schrödinger equation, one is led to a coupled-channel problem, a set of coupled differential equations for the relative-motion wave function $\Psi_{\{\alpha\beta\}}(\vec{r})$. The extremely low collision velocities characteristic of ultracold collisions generally allow one to restrict the set of coupled channels to electronic ground states and the relative motion to the lowest partial waves l only. In addition, symmetry considerations and the associated conservation laws make it possible to group the set of channels into uncoupled subsets.

If at the total energy E the available asymptotic relative kinetic energy in a channel is positive, the channel is called open. Otherwise it is closed. A value of E such that a particular channel opens is a so-called threshold energy. The coupling of the open and closed subspaces of Hilbert space is crucial for the existence of Feshbach resonances. In the following we will be interested in the special features of Feshbach resonances occurring in cold collisions, i.e., close to threshold in a particular collision channel.

III. FESHBACH RESONANCES NEAR THRESHOLD

Two types of resonances play a role in collisions: shape or potential resonances and Feshbach resonances. The first occur when a potential barrier creates quasibound states in the continuum, which after a while decay into a free state. A Feshbach resonance, of most concern in this paper, results when true bound states belonging to a closed channel subspace match the energy of open channels and a coupling exists between them so that temporary transitions are possible during the collision process. The Feshbach theory of resonant states provides a way to calculate the S-matrix element S_{ji} for the transition from an open channel i to another open channel j in the neighborhood of a resonance. We briefly recapitulate the essential steps in order to provide the necessary background needed (a) to understand the special features resulting from the proximity to a channel threshold and (b) to introduce the concepts needed to discuss a modified (strong-field) version of Feshbach theory [11] in Sec. IV C. For a more complete description the reader is referred to the literature [14]. The total Hilbert space describing the spatial and spin degrees of freedom is subdivided into a closed-channel subspace $\mathcal{Q}$, comprising (part of) the closed channels and a complementary open channel subspace $\mathcal{P}$, containing at least the open channels. Feshbach resonances occur as a result of transitions from $\mathcal{P}$ to $\mathcal{Q}$ and back to $\mathcal{P}$ during a collision. Introducing operators P and Q, projecting on $\mathcal{P}$ and $\mathcal{Q}$, the total Schrödinger equation of the system is split into two coupled equations,

$$(E - H_{PP})\Psi_P = H_{PQ}\Psi_Q, \tag{2}$$

$$(E - H_{QQ})\Psi_Q = H_{QP}\Psi_P\ , \tag{3}$$

with $\Psi_P \equiv P\Psi$, $\Psi_Q \equiv Q\Psi$, $H_{PP} \equiv PHP$, $H_{QQ} \equiv QHQ$ and $H_{PQ} \equiv PHQ$.

Equation (3) is formally solved by using the Green operator $\frac{1}{E^+ - H_{QQ}}$, with $E^+ = E + i0$:

$$\Psi_Q = \frac{1}{E^+ - H_{QQ}} H_{QP}\Psi_P\ . \tag{4}$$

Substituting this result in (2) we get

$$(E - H_{\rm eff})\,\Psi_P = 0, \tag{5}$$

where $H_{\rm eff} = H_{PP} + H_{PQ}\frac{1}{E^+ - H_{QQ}}H_{QP}$. The second term in this effective Hamiltonian can be interpreted in terms of a temporary transition from $\mathcal{P}$ space to $\mathcal{Q}$ space, propagation in $\mathcal{Q}$ space, and then reemission into $\mathcal{P}$ space. The next step is expanding the Green operator in discrete eigenstates and (energy normalized) continuum eigenstates of H_{QQ}

$$\frac{1}{E^+ - H_{QQ}} = \sum_m \frac{|\phi_m\rangle\langle\phi_m|}{E - \epsilon_m} + \int d\epsilon \frac{|\phi(\epsilon)\rangle\langle\phi(\epsilon)|}{E^+ - \epsilon}\ . \tag{6}$$

If the total energy E is close enough to a discrete bound state energy ϵ_0 we can forget the remaining terms and (5) reduces to

$$(E - H_{PP})\Psi_P = \frac{H_{PQ}|\phi_B\rangle\langle\phi_B|H_{QP}|\Psi_P\rangle}{E - \epsilon_0}\ , \tag{7}$$

with the formal solution

$$|\Psi_P\rangle = |\Psi_i^+\rangle + \frac{1}{E^+ - H_{PP}}\frac{H_{PQ}|\phi_B\rangle\langle\phi_B|H_{QP}|\Psi_P\rangle}{E - \epsilon_0}\ , \tag{8}$$

where $|\Psi_i^+\rangle$ is an eigenstate of H_{PP} with an incoming wave in channel i. We can solve for $|\Psi_P\rangle$ by multiplication from the left with $\langle\phi_B|H_{QP}$ and find

$$|\Psi_P\rangle = |\Psi_i^+\rangle + \frac{1}{E^+ - H_{PP}}H_{PQ}|\phi_B\rangle \times \frac{\langle\phi_B|H_{QP}|\Psi_i^+\rangle}{E - \epsilon_0 - \langle\phi_B|H_{QP}\frac{1}{E^+ - H_{PP}}H_{PQ}|\phi_B\rangle}\ . \tag{9}$$

The amplitude S_{ji} for the transition to channel j is determined by the asymptotic behavior of Ψ_P

$$S_{ji} = S_{ji}^0 - 2\pi i\frac{\langle\Psi_j^-|H_{PQ}|\phi_B\rangle\langle\phi_B|H_{QP}|\Psi_i^+\rangle}{E - \epsilon_0 - \langle\phi_B|H_{QP}\frac{1}{E^+ - H_{PP}}H_{PQ}|\phi_B\rangle}\ . \tag{10}$$

We see that apart from the "direct" term S_{ji}^0 resulting from coupling within $\mathcal{P}$ space alone, the amplitude of an

outgoing wave in channel j will include a term arising from coupling of the incoming wave in channel i to the bound state in $\mathcal{Q}$ space followed by coupling of this state to channel j. If we have only one open channel i we can write the above expression as

$$S_{ii} = S_{ii}^0 \left(1 - \frac{i\Gamma}{E - \epsilon_0 - \Delta + \frac{i}{2}\Gamma}\right) , \tag{11}$$

where $\Gamma = 2\pi|\langle\phi_B|H_{PQ}|\Psi_i^+\rangle|^2$ represents the width and Δ the so-called resonance shift.

In the case of ultracold collisions of ground state alkali atoms, it is the combination of single-atom hyperfine and Zeeman interactions that determines the threshold of the various channels at the specific magnetic field strength and thus determines the open and closed channel subspaces. The Coulomb interaction force, specifically the exchange part proportional to the difference of singlet and triplet interactions, determines the couplings H_{PQ} and H_{QP} of the open channels to a quasibound closed channel state. Figure 1 shows schematically the energy relationships in $\mathcal{P}$ and $\mathcal{Q}$ space, needed for a Feshbach resonance to show up. For simplicity we have taken both spaces to be one dimensional.

In the foregoing we introduced the orthodox version of Feshbach theory, in which the $\mathcal{P}$ and $\mathcal{Q}$ subspaces are defined in a straightforward way in terms of the sum of the internal atomic Hamiltonians. As a consequence, H_{PQ} does not contain a Zeeman or hyperfine part, but is proportional to $V_S - V_T$. There is therefore no reason to expect H_{PQ} to be a weak perturbation. In the strong-field limit an alternative version of Feshbach's theory can be formulated in which H_{PQ} has a different meaning: essentially the $(\vec{s}_1 - \vec{s}_2)\cdot(\vec{i}_1 - \vec{i}_2)$ part of the total hyperfine interaction, to be denoted as $V_-^{\rm hf}$ in the following [see Eq. (22) below]. This H_{PQ} term represents a weak perturbation in the strong-field limit.

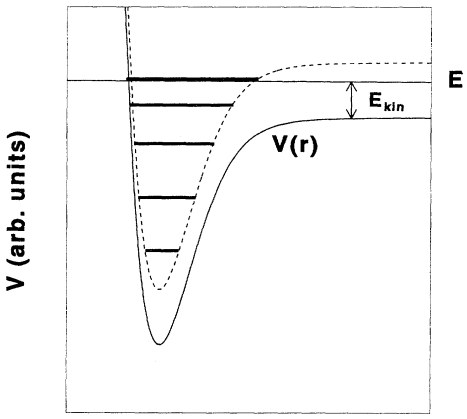

FIG. 1. Coupling between a scattering state and a bound state in a closed channel. The atoms approach each other with total energy E on the potential curve $V(r)$ of the open channel. At a certain kinetic energy the total energy matches that of a bound state (bold line) in the closed channel potential (dashed line).

To formulate this version we note that for strong fields $V_-^{\rm hf}$ plays a negligible role at large interatomic distances, S, M_S, I, M_I being the appropriate, good quantum numbers. It does, however, play a significant role in the radial region of the hyperfine avoided crossings. Effectively therefore we can neglect it beyond a certain distance r_d [11]. In that situation the channel spin states have definite S, M_S, I, M_I and the projection operators P and Q commute with the Coulomb part of the interatomic interaction, so that H_{PQ} is effectively equal to $V_-^{\rm hf}$ instead of being proportional to $V_S - V_T$. This has the important advantage that H_{PQ} is a weak perturbation, which implies that the resonance shift Δ can be expected to be small, so that the position of the resonances will be close to the eigenvalue of $|\phi_0\rangle$ in the isolated $\mathcal{Q}$ space, i.e., neglecting $V^{\rm hf}$. Furthermore, the expression for the resonance width reduces to

$$\Gamma = 2\pi|\langle\phi_0|V_-^{\rm hf}|\Psi_i^+\rangle|^2 \tag{12}$$

in which both $|\phi_0\rangle$ and $|\Psi_i^+\rangle$ are pure singlet or triplet states.

We now specialize the foregoing equations to that of ultralow collision energies. The case that will be of most interest in the following is that of one open channel [Eq. (11)] with both atoms in the same initial spin state, threshold energy $E_{\rm th}$, and collision energy $E_i = E - E_{\rm th}$. At low E_i the surviving s-wave part of Ψ_i^+ is proportional to $\sqrt{k_i} \sim E_i^{1/4}$ in the limited r range of the exchange interaction [15]. As a consequence, expressing the background amplitude in terms of a scattering length a_0, $S_{ii}^0 = e^{-2ik_i a_0}$, Eq. (11) reduces to

$$S_{ii} = e^{-2ik_i a_0}\left(1 - \frac{2iCk_i}{iCk_i - \epsilon_{\rm res}}\right) , \tag{13}$$

where $C > 0$ and $\epsilon_{\rm res} = \epsilon_0 + \Delta(E_i = 0) - E_{\rm th}(B)$ is the actual resonance position relative to threshold. Writing the right-hand side as $e^{-2ik_i a}$, we find for the total scattering length $a(B)$ including the resonance

$$a(B) = a_0 - \frac{C}{\epsilon_{\rm res}} , \tag{14}$$

where a_0 and C are only weakly dependent on B. In practice, the resonance contribution to $a(B)$ shows up only for B values close to the magnetic field strength B_0 where the resonance crosses the threshold. There it is crucial to take the B dependence of $\epsilon_{\rm res}$ into account in the form

$$\epsilon_{\rm res}(B) = [2\mu_i(B_0) - \mu_0(B_0)](B - B_0) \tag{15}$$

with $\mu_i(B)$ the single-atom magnetic moment of the initial hyperfine state and $\mu_0(B)$ the magnetic moment of the two-atom resonance state. We thus have finally

$$a(B) = a_0 - \frac{C}{2\mu_i(B_0) - \mu_0(B_0)}\frac{1}{B - B_0} . \tag{16}$$

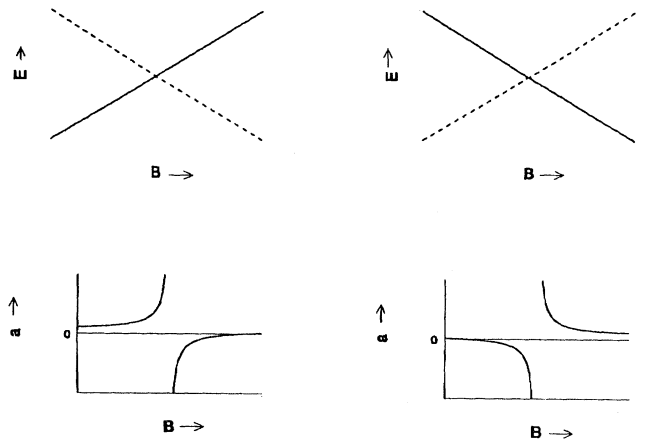

FIG. 2. The two figures on top show the energy of the two-atom resonance state and the channel threshold as a function of B: upper left, for negative magnetic moment of the bound state (solid line) and positive single-atom magnetic moment of the initial hyperfine state (dashed line); upper right, vice versa. The corresponding behavior of the scattering length as a function of magnetic field is shown below. The former situation applies to atoms in the lowest hyperfine state and to strong magnetic fields ($> a_{\rm hf}/\mu_B$) when atoms are in the upper state of the lower hyperfine manifold. The latter situation applies to low magnetic fields for atoms in the upper state of the lower hyperfine manifold. An arbitrary value of a_0 was selected.

Figure 2 illustrates this equation, for both a positive and a negative difference of magnetic moments.

IV. DETERMINATION OF THE LOCATION OF RESONANCES

In this section we describe a calculation that indicates roughly at which magnetic field strengths resonances are expected to occur at threshold. The idea is to calculate the position of discrete two-body states with the appropriate quantum numbers as a function of B, considering the hyperfine coupling as a small perturbation. Comparing these energies with the (B-dependent) threshold energy of the collision channel considered, will give us the desired B values. The effective Hamiltonian of the two-body system is of the form [13,16]

$$H = \frac{\vec{p}^{\,2}}{2\mu} + \sum H^{\rm int} + V^c + V^d \ , \tag{17}$$

where $\sum H^{\rm int}$ represents the internal energy of the two atoms, i.e., the sum of the hyperfine and Zeeman interactions, V^c is the central (Coulomb) interaction, and V^d the magnetic dipole interaction. Previous studies [12,17] indicate that an effective Hamiltonian of this form provides for a description of observable quantities to the percent or even promille level.

The central interaction depends only on $|\vec{r}|$ and therefore conserves orbital angular momentum l and total spin F ($\vec{F} = \vec{S} + \vec{I}$, where $\vec{S}$ stands for the total electron spin and $\vec{I}$ is the total nuclear spin), as well as their projections m_l and M_F. It also conserves $\vec{S}$ and $\vec{I}$ separately and can be decomposed in singlet and triplet terms

$$V^c = V_0(r)P_0 + V_1(r)P_1 \ , \tag{18}$$

where the P_S operator projects on the singlet $S = 0$ or triplet $S = 1$ subspace. The dipole interaction, on the other hand, is not invariant under independent rotations of spatial and spin degrees of freedom as it depends on relative orientations in space of orbital and spin degrees of freedom and thus may change F and M_F. Since the dipole interaction is much weaker than the central interaction, however, and since we are not interested in dipolar rates here, we will neglect this term in the following.

The internal Hamiltonian of a single atom is taken to be

$$H^{\rm int} = \frac{a_{\rm hf}}{\hbar^2}\vec{s}\cdot\vec{i} + (\gamma_e s_z - \gamma_n i_z)\, B_z \ , \tag{19}$$

where $a_{\rm hf}$ is the hyperfine constant, $\vec{s}$ is the electronic spin, and $\vec{i}$ is the nuclear spin. The first term is the hyperfine interaction and the second is the Zeeman interaction. The energy levels of atoms with nuclear spin $i = \frac{3}{2}$ and $i = 1$ are shown in Fig. 3. We will label the one-atom hyperfine states with $|f, m_f\rangle$, where $\vec{f} = \vec{i} + \vec{s}$, although f is a good quantum number only for $B = 0$. Asymptotically the central interaction can be neglected and the two-body system is described by the eigenstates of each of the atoms separately. The scattering channels at infinity are therefore labeled as $|\{f_1 m_{f_1}, f_2 m_{f_2}\}^{\pm}\rangle$, with + denoting the symmetrized and − the antisymmetrized spin states: depending on the orbital angular quantum number l and the atomic species (^{7}Li and ^{23}Na behave as bosons, ^{6}Li as a fermion) symmetrized or antisymmetrized spin states are needed. For small r values it is more convenient to use a basis that exploits the fact that the central interaction is much stronger than the hyperfine or Zeeman interaction. Depending on the strength of the magnetic field the set $|(SI)FM_F\rangle$ or the set $|SM_SIM_I\rangle$ offers more advantages. In Fig. 4 we give an example of the adiabatic energy curves together with their labels in the two different regions of r. In between these regions neither of the sets is a "good" diagonal basis set; the adiabatic states will be mixtures of different basis states.

A. Singlet and triplet potentials

In a previous paper [18] we have shown how we have improved the Li triplet potential, obtained by Zemke and Stwalley [19] via a "dense" Rydberg-Klein-Rees (RKR) analysis of spectroscopic data and the addition of short and long range analytical parts, by inverse perturbation analysis (IPA). Recent measurements [5] support the quality of this IPA potential. We have also been able to

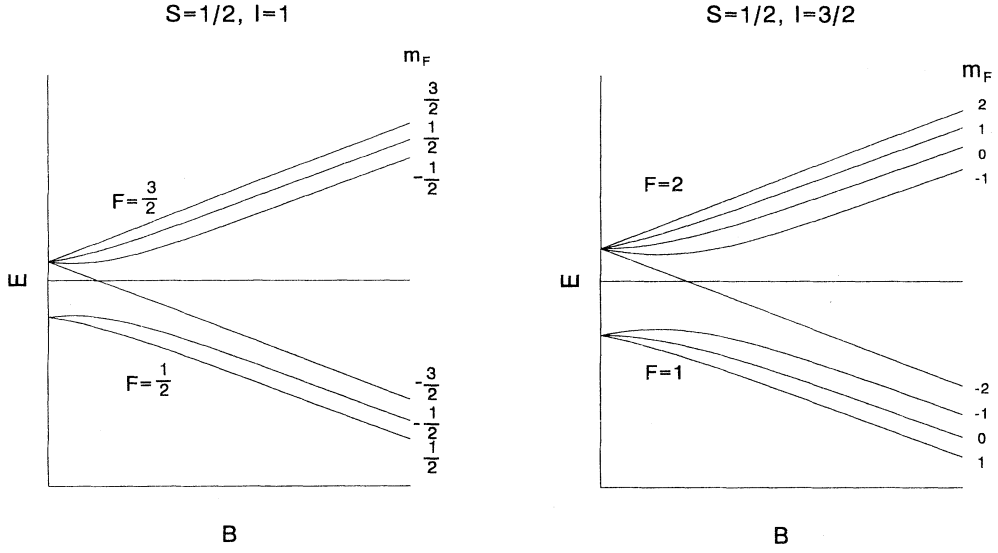

FIG. 3. Energies of hyperfine states, labeled $|FM_F\rangle$, as a function of magnetic field, for atoms with nuclear spin $i = 1$ and $i = \frac{3}{2}$ (E and B scales are in arbitrary units).

find the uncertainty left in the triplet as well as in the singlet potential [18,20]. In the case of Na we started from the state of the art potentials from Refs. [21,22]. We further improved the Na singlet interaction with IPA. Unfortunately, there are insufficient experimental data to also improve the Na triplet potential. To get an idea of the remaining error in the potentials we look at the phase mismatch $\phi(E,l)$ at a suitable meeting point of small-r and large-r parts of the wave function obtained by outward and inward integration of the Schrödinger equation. $\phi(E,l)$ is expected to be zero at the energy of a bound state. In the WKB approximation, with $k = k_{E,l}(r)$ the local wave number and $r_1(E,l)$ and $r_2(E,l)$ the inner and outer turning points, the error is given by

$$\Delta\phi(E,l) = \int_{r_1}^{r_2} \Delta k(r)dr \ . \tag{20}$$

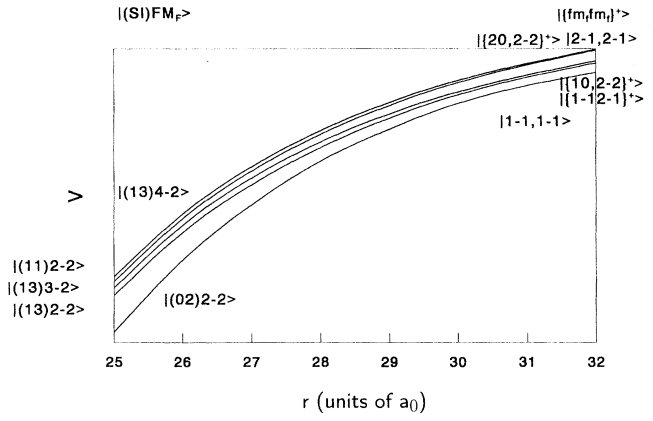

FIG. 4. ^{23}Na+^{23}Na adiabatic energy curves for zero magnetic field. For small r values the states are labeled $|(SI)FM_F\rangle$ and for large r values the curves are described by the eigenstates of the internal Hamiltonian of each of the atoms separately.

Differentiation of this quantity with respect to E and $l(l+1)$ emphasizes the dependence on the contribution from an interval close to the outer turning point where the "classical" motion is slow and the potential is already more reliable. It is therefore plausible [18,20] that the derivatives of $\phi(E,l)$ with respect to E and $l(l+1)$ are already described accurately by the present best singlet and triplet potentials and to allow only for a shift $\Delta\phi(0,0)$ at $E = l = 0$. By looking at the discrepancies between the experimental and calculated energy differences of the highest measured bound states as a function of this shift for the ^{7}Li singlet and triplet potential the following ranges were found [18,20]:

$$-0.02 < \Delta\phi_{S=0} < 0.05, \quad -0.04 < \Delta\phi_{S=1} < 0.035 \ .$$

For ^{6}Li we adopt the same ranges. This is justified by the fact that our ^{7}Li IPA curve differs only slightly from the ^{6}Li dense RKR curve, which indicates that adiabatic corrections are small. It should be noted that the above uncertainty in the shift is small, only a few percent of the period π, confirming the quality of the potentials.

Recently the highest $l = 0$ bound state of ^{7}Li triplet has been measured and was found at a distance of 598 $\pm$ 2 mK below the continuum [5]. This measurement completely pins down the position of the ^{7}Li triplet resonances, as will be shown in the following.

That the above mentioned phase method can also be used to improve the potentials is illustrated by the Na singlet interaction. In Fig. 5 the discrepancies between experimental [23] and calculated energy differences for the highest measured rovibrational levels as a function of the shift $\Delta\phi$ for the Na singlet potential, which we obtained by the IPA, are shown. Clearly the shift $\Delta\phi$ for $E_{v=62,J} - E_{v=61,J}$, which are the highest measured levels, is significant. However, according to Ref. [21] the outermost RKR turning point is subject to a relatively large uncertainty. Figure 6 shows the $\Delta E - \Delta\phi$ diagram that we obtained after a suitable shift of this point. Appar-

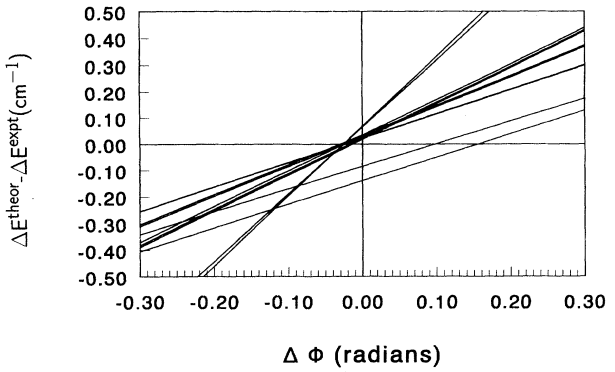

FIG. 5. Discrepancies between measured and calculated energy differences (left axis, solid lines) for the Na singlet potential as a function of $\Delta\phi$. The $(v+1,J)$-(v,J) combinations for the lines from top to bottom at $\Delta\phi = 0.3$ are (59,15)-(57,15), (59,13)-(57,13), (57,13)-(56,13), (57,15)-(56,15), (56,15)-(55,15), (60,13)-(59,13), (60,15)-(59,15), (61,15)-(60,15), (61,13)-(60,13), (62,13)-(61,13), and (62,15)-(61,15).

ently, the shift of this single RKR turning point brings the intersection points with the abscissa remarkably close together. We thus find the following ranges for the phase shift:

$$-0.04 < \Delta\phi_{S=0} < 0.00, \quad -0.3 < \Delta\phi_{S=1} < 0.3 \ .$$

Compared to the other potentials mentioned above, the uncertainty in the Na triplet interaction is rather large due to the fact that only a relatively small number of bound levels for this state has been measured, with a rather low resolution. However, recent measurements of the elastic cross section of Na atoms in the $F = 1, m_F = -1$ state [2] give an elastic scattering length $[\pm(92 \pm 25)a_0]$ that is close to the middle of the interval where

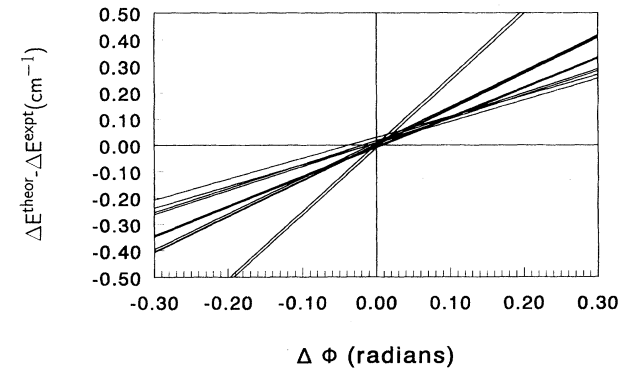

FIG. 6. Discrepancies between measured and calculated energy differences (left axis, solid lines) for the Na singlet as a function of $\Delta\phi$ after shifting the outermost RKR point. The $(v+1,J)$-(v,J) combinations for the lines from top to bottom at $\Delta\phi = 0.3$ are (59,15)-(57,15), (59,13)-(57,13), (57,13)-(56,13), (56,13)-(55,13), (57,15)-(56,15), (56,15) -(55,15), (60,15)-(59,15), (60,13)-(59,13), (61,15)-(60,15), (61,13)-(60,13), (62,13)-(61,13), and (62,15)-(61,15).

we predicted it to be $(64 < a_{1-1} < 152a_0)$. This points to the fact that the uncertainty in the triplet potential given above is rather overestimated.

Apart from the errors in the "inner" parts of the potentials the dispersion coefficients C_6, C_8, C_{10} too have certain error bounds. These errors may move the analytical part of the potential curve up or down relative to the bottom and thus affect the positions of the energy levels. To determine the effect of this uncertainty in the potential on the bound state energy levels, the experimental data points were shifted to match the maximum and minimum analytical tails, respectively. Calculating the positions of the presently unknown (except the ^{7}Li triplet) highest two-body energy levels in the following, we will take into account the combined effect of the uncertainties in the long range part and in the inner part of the potentials.

B. Bound state energy levels

The method we now follow to find the bound levels will consist of calculating the energy of the highest bound levels of the singlet $S = 0$ and triplet $S = 1$ ground states and include the hyperfine and Zeeman interaction

$$\sum H^{\rm int} = \frac{a_{\rm hf}}{\hbar^2}\left(\vec{s}_1\cdot\vec{i}_1 + \vec{s}_2\cdot\vec{i}_2\right) + (\gamma_e S_z - \gamma_n I_z)\,B_z \ . \tag{21}$$

Neglecting the mixing of different (SI) combinations by the $(\vec{s}_1-\vec{s}_2)\cdot(\vec{i}_1-\vec{i}_2)$ part of the total hyperfine interaction

$$\begin{aligned}\frac{a_{\rm hf}}{\hbar^2}\left(\vec{s}_1\cdot\vec{i}_1 + \vec{s}_2\cdot\vec{i}_2\right) &= \frac{a_{\rm hf}}{2\hbar^2}\,(\vec{s}_1+\vec{s}_2)\cdot\left(\vec{i}_1+\vec{i}_2\right) \\ &\quad + \frac{a_{\rm hf}}{2\hbar^2}\,(\vec{s}_1-\vec{s}_2)\cdot\left(\vec{i}_1-\vec{i}_2\right) \\ &\equiv V_+^{\rm hf} + V_-^{\rm hf} \ ,\end{aligned} \tag{22}$$

these states are characterized in the zero-field limit by the total spin and the total spin-projection quantum numbers F and M_F and are written as $|v, l(SI)FM_F\rangle$.

This approximation is justified except for very close-lying singlet and triplet levels (within a distance of about $a_{\rm hf}$). Note that $\vec{s}_1 - \vec{s}_2$, being antisymmetric in 1 and 2, couples symmetric (i.e., triplet) electronic spin states and antisymmetric (i.e., singlet) states. Due to the differences in electronic and nuclear gyromagnetic ratios, as an external magnetic field is applied, bound states will be mixtures of various $|(SI)FM_F\rangle$ states with different F. For very strong fields each of the eigenstates approaches a state with definite total electronic spin (S and M_S) and total nuclear spin (I and M_I), so that in this limit these are the good quantum numbers. These basis states are denoted as $|SM_SIM_I\rangle$ and the bound states are likewise characterized by $|v, lSM_SIM_I\rangle$.

We illustrate the above by considering two Na atoms in the $|f = 1, m_f = -1\rangle$ state. In this case we have two atoms in the same spin state, requiring that l be even to form a symmetric total wave function. In all cases, symmetry considerations require that the sum $l + I + S$

be even. Note that this rule applies to both bosonic and fermionic alkali atoms: the permutation symmetry of the electronic spin states is determined by $(-1)^{1-S}$, and that of the nuclear spin states by $(-1)^{2i-I}$. From the above requirement of even l, we thus have $S+I$ even for ^{23}Na. Taking into account that the (conserved) total $M_F=-2$, so that $F \geq 2$, we have the possibilities

$$S=1 \rightarrow \begin{cases} I=1 \rightarrow & F=2 \\ I=3 \rightarrow & F=2,3,4 \end{cases},$$
$$S=0 \rightarrow \quad I=2 \rightarrow \quad F=2 .$$

The structure of these four triplet and one singlet states is easily derived, both in the weak-field and strong-field limits, provided we write the hyperfine interaction in the approximation explained above as $V_{+}^{\mathrm{hf}}=\frac{a_{\mathrm{hf}}}{2\hbar^2}\vec{S}\cdot\vec{I}$. Clearly, this term conserves S, I, F, M_F. Since the same is true for the Coulomb part of the interatomic interaction, this determines the set of good quantum numbers in the zero-field (and weak-field) limit. As pointed out above, the external field does not conserve F. It does conserve S, M_S, I, M_I however. This defines the set of good quantum numbers in the strong-field limit. We conclude that in the $\vec{S}\cdot\vec{I}$ approximation the problem of finding the two-body bound states can be solved in terms of uncoupled orbital and spin states. The orbital problem leads to a set of eigenstates in a pure singlet or triplet potential, the spin problem to the states

Weak B field		Strong B field
$\|(SI)FM_F\rangle$		$\|SM_SIM_I\rangle$
$\|(02)2-2\rangle$	$\rightarrow$	$\|002-2\rangle$
$\|(11)2-2\rangle$	$\rightarrow$	$\|1-11-1\rangle$
$\|(13)2-2\rangle$		$\|1-13-1\rangle$
$\|(13)3-2\rangle$	$\rightarrow$	$\|103-2\rangle$
$\|(13)4-2\rangle$		$\|113-3\rangle$

for extreme fields and easily calculable superpositions for intermediate field strengths. For each orbital state, a multiplet of spin levels is thus obtained by calculating the matrix elements of the internal Hamiltonian in the $|(SI)FM_F\rangle$ basis and diagonalizing this matrix. Figure 7 shows the energies of the $v=14, l=0$ triplet and $v=65, l=0$ singlet bound states. Also shown is the open channel threshold energy of the $|1-1,1-1\rangle$ collision channel. It is seen that there is reason to expect resonant behavior at magnetic field values of $B=0.105$ T and $B=0.185$ T.

A rigorous way to find the exact location of the resonances is to solve the coupled-channel equation numerically. The result is obtained in the form of the S-matrix elements. Rapid change in an S-matrix element indicates a resonance. With a single channel open, elastic S-matrix elements can be written as $e^{2i\delta(k)}$, where δ is known as the phase shift and k stands for the wave number. A quantity of crucial importance for the achievement of Bose-Einstein Condensation (BEC) is the so-called scattering length a, defined as $a=-\lim_{k\rightarrow 0}\delta(k)$. Figure 8 shows the value of the scattering length for the collision of two atoms in the $|f=1, m_f=-1\rangle$ state following from a rigorous coupled-channel calculation. Clearly, we find perfect agreement of the resonance positions obtained from

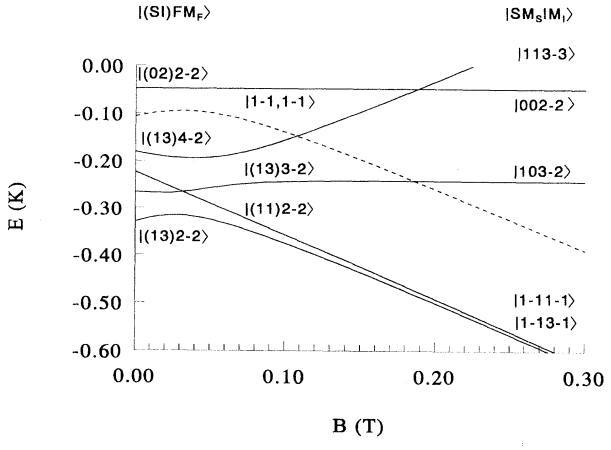

FIG. 7. Energies of the singlet (S=0) $v=65, l=0$ and triplet (S=1) $v=14, l=0$ bound states as a function of magnetic field. At B=0 the degeneracy of the triplet state is lifted by the hyperfine interaction. Also shown (dashed line) is the threshold energy of the $|1-1,1-1\rangle$ collision channel. Resonances occur when this line intersects a bound state curve.

the simple bound state model and the positions from the coupled-channel calculations.

It is of importance to point to a basic difference of the present calculations with those of Ref. [6]: for ^{23}Na and for the Li isotopes we now have detailed knowledge of the relevant properties of singlet and triplet potentials available, so that our theoretical results do not represent order of magnitude estimates but rather accurate predictions with narrow error limits. As stated before, uncertainties in the potentials will shift the bound state levels up or down, resulting in a shift of the position of the resonance. Taking account of the uncertainties left over for the Na potentials we find the resonance position at $0.084 < B < 0.134$ T. In Table I we summarize the calculations along similar lines for ^{6}Li, ^{7}Li, and ^{23}Na. We only consider states that are stable against exchange relaxation. Note that all resonances are predicted at field values large relative to a_{hf}/μ_B, where the strong-field limit is valid.

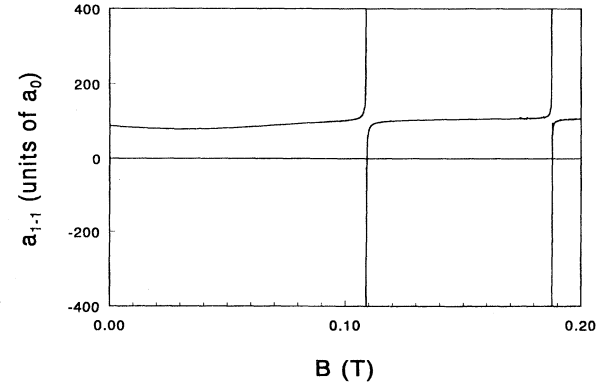

FIG. 8. Value of scattering length for the f=1, $m_f=-1$ state as a function of magnetic field following from the coupled-channel calculation.

TABLE I. Location of resonances for different atoms, different entrance channels, and various bound states (indicated by quantum numbers at zero magnetic field) from which the resonances result.

Atom	$\|fm_f\rangle$ state	$B_{\rm res}$	Bound state
^{6}Li	$\|\frac{1}{2}-\frac{1}{2}\rangle$	11.7 mT $< B <$ 26.5 mT	$\|38,1,(01)1-1\rangle$
		0.337 T $< B <$ 0.384 T	$\|9,1,(12)3-1\rangle$
	$\|\frac{1}{2}\frac{1}{2}\rangle$	6.4 mT $< B <$ 21.0 mT	$\|38,1,(01)11\rangle$
		0.332 T $< B <$ 0.382 T	$\|9,1,(12)31\rangle$
		0.332 T $< B <$ 0.382 T	$\|9,1,(10)11\rangle$
^{7}Li	$\|1-1\rangle$	0.078 T $< B <$ 0.137 T	$\|41,0,(02)2-2\rangle$
		0.233 T $< B <$ 0.237 T	$\|10,0,(13)4-2\rangle$
	$\|11\rangle$	0.052 T $< B <$ 0.082 T	$\|41,0,(02)22\rangle$
		0.205 T $< B <$ 0.209 T	$\|10,0,(13)42\rangle$
		0.205 T $< B <$ 0.209 T	$\|10,0,(11)22\rangle$
^{23}Na	$\|1-1\rangle$	0.084 T $< B <$ 0.134 T	$\|14,0,(13)4-2\rangle$
		0.148 T $< B <$ 0.172 T	$\|14,0,(13)3-2\rangle$
	$\|11\rangle$	0.016 T $< B <$ 0.068 T	$\|14,0,(13)42\rangle$
		0.03 T $< B <$ 0.075 T	$\|14,0,(11)22\rangle$
		0.09 T $< B <$ 0.185 T	$\|14,0,(10)32\rangle$

C. Resonance widths

In the preceding subsection we found the locations of the resonances corresponding to the singlet and triplet closed channel bound states. We will now concern ourselves with their widths. We want to predict these in the strong-field limit, which, as we have seen, turns out to apply for all predicted ^{6}Li, ^{7}Li, and ^{23}Na resonances. In that limit it is profitable to adopt the modified version of Feshbach's theory considered above, leading to Eq. (12) for the width. Since we know the closed channel bound state $|\phi_0\rangle$ to be a pure singlet or pure triplet state, its wave function can be determined by numerical integration of the Schrödinger equation. In order to evaluate (12), we will need to look more closely at the scattering state $|\Psi_i^+\rangle$ in the case of a low-energy collision between ground state atoms. In the following we will take the specific singlet resonance of ^{6}Li in the $|f=\frac{1}{2},m_f=-\frac{1}{2}\rangle$ state as an example. The two-atom combinations that give a total magnetic quantum number $M_F=-1$ form a five-dimensional spin subspace. These states can be expressed in the convenient $|SM_SIM_I\rangle$ basis. The mixture of $|SM_SIM_I\rangle$ states in the entrance channel spin state $|f=\frac{1}{2},m_f=-\frac{1}{2},f=\frac{1}{2},m_f=-\frac{1}{2}\rangle$ is

$$
\begin{aligned}
&|\{\tfrac{1}{2}-\tfrac{1}{2},\tfrac{1}{2}-\tfrac{1}{2}\}^+\rangle \\
&\quad=\beta^2|112-2\rangle+\sqrt{\frac{2}{3}}\alpha^2|1-120\rangle-\alpha\beta|102-1\rangle \\
&\qquad-\frac{1}{\sqrt{3}}\alpha^2|1-100\rangle+\alpha\beta|001-1\rangle\,, \qquad (23)
\end{aligned}
$$

where

$$
\begin{aligned}
\alpha&=\cos\Theta,\\
\beta&=\sin\Theta,\\
\Theta&=\frac{1}{2}\arctan\left(\frac{2\sqrt{2}}{1+2(\gamma_e+\gamma_n)\frac{\hbar}{a}B}\right).
\end{aligned}
$$

From these expressions it is seen that the singlet contribution vanishes for large values of the field. At large fields the state is a mixture of the triplet states $|1-120\rangle$ and $|1-100\rangle$. This confirms the assumption of pure singlet or triplet channel spin states in the modified Feshbach theory. Since $V_-^{\rm hf}$ couples the above triplet channels to $S=0$ only, we can expect resonances with only very narrow widths for triplet bound states, which will probably be very difficult to observe. This again is confirmed by the rigorous results for the resonances obtained with our coupled-channel calculations. The resonance width for a singlet bound state, on the other hand, is determined by Eq. (12) taking the form

$$\Gamma=2\pi|\langle\phi_{S=0}|V_-^{\rm hf}|\Psi_{S=1}^+\rangle|^2, \qquad (24)$$

where $\phi_{S=0}$ is the singlet bound state and $\Psi_{S=1}^+$ is a triplet scattering state, i.e., a p-wave continuum wave function. Working out spin matrix elements we finally get

$$\Gamma=2\pi\frac{a_{\rm hf}^2}{2}\left(\int d\vec{r}\phi_{S=0}(\vec{r})\Psi_{S=1}(\vec{r})\right)^2, \qquad (25)$$

with $\phi_{S=0}(\vec{r})$ and $\Psi_{S=1}(\vec{r})$ the spatial parts of the bound and scattering wave functions. We conclude that the bound state has to be a p-wave state too. Numerical integration of (25) yields the resonance widths as a function of collision energy. In Table II these are compared to the values resulting from a rigorous numerical solution of the coupled-channel equations. The agreement between the two is good, justifying our strong-field approximation and modified Feshbach theory.

The energy dependence seen in the table is of the form $E^{3/2}$ and is due to the scattering wave function Ψ. This can be seen from the low-energy behavior of the free part of the radial wave function

$$\sqrt{kr}j_l(kr)\to\frac{1}{\sqrt{k}}\frac{(kr)^{l+1}}{(2l+1)!!}\,. \qquad (26)$$

Thus the width goes with $E^{l+1/2}$. Figure 9 shows the dependence of the width on E and Fig. 10 shows the B dependence for different energies. Note the ideal Breit-Wigner shape of the resonances due to the fact that the

TABLE II. Resonance widths of the ^{6}Li singlet resonance for collision energies, calculated with the modified Feshbach theory ($\Gamma^{\rm Fesh}$) and with the coupled-channel calculation ($\Gamma^{\rm cc}$).

E (mK)	$\Gamma^{\rm Fesh}$ (mK)	$\Gamma^{\rm cc}$ (mK)
0.25	0.0094	0.010
0.50	0.026	0.030
1.00	0.074	0.081
2.00	0.20	0.22

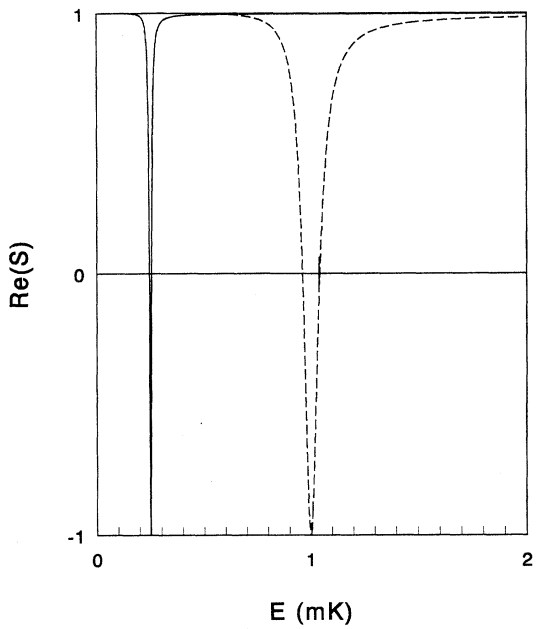

FIG. 9. Energy dependence of real part of the S-matrix element at the magnetic field giving a resonance at 0.25 mK (dashed curve) and at 1 mK.

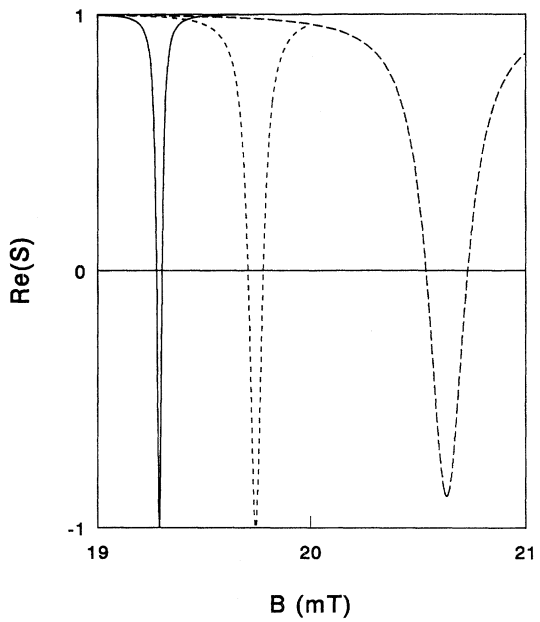

FIG. 10. B dependence of real part of the S-matrix element with a kinetic energy of 0.5 mK (dashed), 1 mK (dotted), and 2 mK in the incoming channel.

nonresonant phase shift is zero.

We now turn to a calculation of the widths of the complete set of resonances obtained by the rigorous coupled-channel calculation. Table III summarizes the widths of the resonances from Table I along the B scale for kinetic energies of 1 μK and 10 μK in the corresponding scattering channel. The table shows a large variation in width for different resonances. Small widths can be explained by the fact that the interaction is not efficient in coupling the entrance channel with a quasibound state. An example is the resonance corresponding to the bound state $|10,0\ (13)4-2\rangle$ for ^{7}Li. In the B-field region where the resonance is found the entrance channel is almost a pure triplet. The bound state is also an $S=1$ state. The $V_-^{\rm hf}$ part of $V^{\rm hf}$, however, couples only triplet with singlet states.

V. CONCLUSION

We conclude that the hope of predicting resonance phenomena in the low-field seeking region for the highest states of the lower hyperfine manifold for ^{6}Li, ^{7}Li, and

TABLE III. The widths of the resonances from Table I. The widths of the ^{6}Li triplet resonances were too small for these low energies to be calculated. We found a width of 16×10^{-6} for a kinetic energy of 10 mK. The ampersand denotes that this bound state overlaps the previous one so that no separate widths could be determined.

Atom	$\lvert fm_f\rangle$ state	Bound state	ΔB (G) for $E_{\rm kin}=1$ μK	ΔB (G) for $E_{\rm kin}=10$ μK
^{6}Li	$\lvert\frac{1}{2}-\frac{1}{2}\rangle$	$\lvert 38,1(01)1-1\rangle$	0.000025	0.0008
		$\lvert 9,1(12)3-1\rangle$		
	$\lvert\frac{1}{2}\frac{1}{2}\rangle$	$\lvert 38,1(01)11\rangle$	0.000025	0.0008
		$\lvert 9,1(12)31\rangle$		
		& $\lvert 9,1(10)11\rangle$		
^{7}Li	$\lvert 1-1\rangle$	$\lvert 41,0(02)2-2\rangle$	1.22	3.84
		$\lvert 10,0(13)4-2\rangle$	0.001	0.004
	$\lvert 11\rangle$	$\lvert 41,0(02)22\rangle$	0.85	2.7
		$\lvert 10,0(13)42\rangle$	0.002	0.006
		& $\lvert 10,0(11)22\rangle$		
^{23}Na	$\lvert 1-1\rangle$	$\lvert 14,0(13)4-2\rangle$	0.20	0.63
		$\lvert 14,0(13)3-2\rangle$	0.094	0.30
	$\lvert 11\rangle$	$\lvert 14,0(13)42\rangle$	0.0008	0.0026
		$\lvert 14,0(11)22\rangle$	0.45	1.48
		$\lvert 14,0(10)32\rangle$	0.038	0.123

^{23}Na is apparently not fulfilled. It should be noted, however, that the predicted resonances might be observable with recently proposed and developed trapping schemes [8–10]. We have found the positions of these resonances and calculated their widths. Exciting phenomena may be expected to take place in a trap at locations where the field value corresponds to a resonance. In addition, the observation of these resonances in such an experiment would provide a measure of the quality of the interatomic potentials derived in our group and reduce the uncertainty associated with them.

ACKNOWLEDGMENT

This work is part of a research program of the Stichting voor Fundamenteel Onderzoek der Materie, which is financially supported by the Nederlandse Organisatie voor Wetenschappelijk Onderzoek.

[1] N.R. Newbury, C.J. Myatt, E.A. Cornell, and C.E. Wieman, Phys. Rev. Lett. **74**, 2196 (1995).

[2] K.B. Davis, M.O. Mewes, M.A. Joffe, M.R. Andrews, and W. Ketterle (unpublished).

[3] M.S. Shahriar, P.R. Hemmer, M.G. Prentiss, P. Marte, J. Mervis, D.P. Katz, N.P. Bigelow, and T. Cai, Phys. Rev. A **48**, R4035 (1993).

[4] J.R. Gardner, R.A. Cline, J.D. Miller, D.J. Heinzen, H.M.J.M. Boesten, and B.J. Verhaar (unpublished).

[5] E.R.I. Abraham, W.I. McAlexander, C.A. Sackett, and R.G. Hulet, Phys. Rev. Lett. **74**, 1315 (1995).

[6] E. Tiesinga, B.J. Verhaar, and H.T.C. Stoof, Phys. Rev. A **47**, 4114 (1993).

[7] N.R. Newbury, C.J. Myatt, and C.E. Wieman, Phys. Rev. A (to be published).

[8] R.J.C. Spreeuw, C. Gerz, L.S. Goldner, W.D. Phillips, S.L. Rolston, C.I. Westbrook, M.W. Reynolds, and I.F. Silvera, Phys. Rev. Lett. **72**, 3162 (1994).

[9] J.D. Miller, R.A. Cline, and D.J. Heinzen, Phys. Rev. A **47**, R4567 (1993).

[10] T. Takekoshi, J.R. Yeh, and R.J. Knize, Opt. Commun. **114**, 421 (1995).

[11] The formulation of this alternative version of Feshbach theory without the motivation given here was presented by J. Dohmen, B.J. Verhaar, and J.M.V.A. Koelman, Eindhoven University Report, 1987 (unpublished).

[12] R.M.C. Ahn, J.P.H.W. van den Eijnde, and B.J. Verhaar, Phys. Rev. B **27**, 5424 (1983).

[13] H.T.C. Stoof, J.M.V.A. Koelman, and B.J. Verhaar, Phys. Rev. B **38**, 4688 (1988).

[14] See, for instance, H. Feshbach, *Theoretical Nuclear Physics* (Wiley, New York, 1992).

[15] John R. Taylor, *Scattering Theory* (Wiley, New York, 1972).

[16] E. Tiesinga, A.J. Moerdijk, B.J. Verhaar, and H.T.C. Stoof, Phys. Rev. A **46**, R1167 (1992).

[17] J.P.H.W. van den Eijnde, Ph.D. thesis, Eindhoven University of Technology, 1984 (unpublished).

[18] A.J. Moerdijk, W.C. Stwalley, R.G. Hulet, and B.J. Verhaar, Phys. Rev. Lett **72**, 40 (1994).

[19] W.T. Zemke and W.C. Stwalley, J. Chem. Phys. **97**, 2053 (1993).

[20] A.J. Moerdijk and B.J. Verhaar, Phys. Rev. Lett. **73**, 518 (1994).

[21] W.T. Zemke and W.C. Stwalley, J. Chem. Phys. **100**, 2661 (1994).

[22] There are a few typographical errors in Table II of Ref. [21]. The $G(v)$ value for $v = 26$ should read 3665.2574 instead of 3655.2574 and the last $G(v)$ value in the table should read 6021.5453 instead of 6021.5553.

[23] R.F. Barrow, J. Verges, C. Effantin, K. Hussein, and J. d'Incan, Chem. Phys. Lett. **104**, 179 (1984).

[24] (a) The condition of a strong elastic scattering cross section for evaporative cooling was mentioned by Wieman in 1992 (C.E. Wieman, private communication) and was later published in (b). In Ref. [20] we pointed out that $\sigma_{\rm el}(T \to 0) = 8\pi a^2$ goes through ∞ near a Feshbach resonance, so then the condition can be realized for suitable B. (b) C. Monroe, E.A. Cornell, C.A. Sacket, C.J. Myatt, and C.E. Wieman, Phys. Rev. Lett. **70**, 414 (1993).